

Brief Report

Lu–Hf Geochronology on Single Garnets in a Micaschist from the North Qilian Orogenic Belt

Chi Cao and Hao Cheng *

State Key Laboratory of Marine Geology, Tongji University, Shanghai 200092, China

* Correspondence: chenghao@tongji.edu.cn; Tel.: +86-21-6598-1305

Abstract: The acquisition of the timing and duration of metamorphic mineral growth is the key to understanding the evolution of metamorphic belts. Garnet Lu–Hf geochronology is becoming increasingly powerful in this aspect. It is believed that garnet Lu–Hf radiometric systems are preserved during low-temperature metamorphism. However, this hypothesis has not been systematically tested. To examine the Lu–Hf systematics of garnets during low-temperature metamorphism, we conducted radiometric dating on individual garnet crystals of different sizes from a single micaschist in the North Qilian orogenic belt. The garnet Lu–Hf dates correlate well with the grain sizes and their core Mn concentrations. The positive correlation between the ages and grain sizes suggests that grain size is a proxy for preserving garnet nucleation and growth history. Small grains nucleated and grew later than large crystals. The Lu–Hf date of the individual garnet crystals faithfully recorded the total growth time span. The date difference of ~16 Myr is the minimum duration of the total garnet growth. The age discrepancy between the micaschist and the eclogite indicates they may not have experienced the same subduction and exhumation in the North Qilian orogenic belt.

Keywords: Lu–Hf; single garnet; Qilian

1. Introduction

Gaining insight into the duration and timing of mineral growth during metamorphism is crucial for comprehending the metamorphic process. Garnet is an invaluable key mineral for determining the temporal P – T conditions of a range of metamorphic processes due to its ability to commonly preserve a record of chemical variation across a broad spectrum of metamorphic grades. Its compositional variations can be utilized to accurately determine P – T constraints, which can be directly linked to precise Sm–Nd and Lu–Hf ages [1]. Thus, garnet geochronology has rightfully attracted broad interest. In addition, garnet Lu–Hf dating has become an indispensable approach to gain insights into the early stage of metamorphic processes due to the high affiliation of Lu in garnet that may lead bulk garnet dates to skew to early growth, resulting in older Lu–Hf dates than Sm–Nd dates of the same garnet fragment. However, such bias may result from a presumably higher closure temperature (T_c) for Lu–Hf than Sm–Nd in high-temperature rocks that tend to be eliminated/dislocated by later thermal overprint [2,3].

During metamorphic garnet growth, certain elements, such as Mn and Lu, are preferentially incorporated into the growing crystal. This leads to chemically zoned porphyroblast garnets due to the progressive depletion of Mn/Lu in the surrounding matrix. Therefore, the elemental and isotopic chemical variations in the garnet provide a spatial and temporal record of the progressive metamorphism over which the garnet grew. Hypothetically, in low-temperature metamorphic rocks where major elements and isotopes in the garnet are not significantly re-equilibrated by diffusion, garnet nucleation and growth may be faithfully preserved. Garnets, which nucleate first and maintain a longer record of metamorphism, may exhibit an older Lu–Hf date than those that form later in the metamorphic process. Therefore, as an indicator component for the nucleation and growth of garnet,



Citation: Cao, C.; Cheng, H. Lu–Hf Geochronology on Single Garnets in a Micaschist from the North Qilian Orogenic Belt. *Minerals* **2023**, *13*, 276. <https://doi.org/10.3390/min13020276>

Academic Editor: Alexey V. Ivanov

Received: 10 January 2023

Revised: 13 February 2023

Accepted: 14 February 2023

Published: 15 February 2023



Copyright: © 2023 by the authors. Licensee MDPI, Basel, Switzerland. This article is an open access article distributed under the terms and conditions of the Creative Commons Attribution (CC BY) license (<https://creativecommons.org/licenses/by/4.0/>).

the Mn concentration in the garnet core is expected to correlate with the Lu–Hf ages of individual garnet crystals in such metamorphic rocks.

The most straightforward and ideal way to test this hypothesis is to use the newly developed in situ laser-ablation high-spatial-resolution Lu–Hf method [4] to date individual zoned garnets. However, thus far, this method's rapid analysis produces less precise dates than conventional solution methods, making the date differences between the distinct zones indistinguishable within analytical uncertainties. Another way to test this hypothesis is through the use of high-spatial-resolution microsampling methods, such as microdrill/microsaw and laser cutting. This allows for acquiring high-resolution and high-precision Lu–Hf geochronological dates in distinct growth shells from the core to the rim in a single garnet [5,6]. This method, however, is strictly limited to several cm-sized garnet grains due to sample size requirements. Dissolving a "common" mm-sized garnet in high-grade metamorphic rock barely yields a sufficient amount of Hf for a precise isotope dilution analysis with conventional multi-collector- (MC-) ICP-MS due to the low Hf concentrations. Feasible alternatives include dating a number of drilled garnet cores [5] or dissolving a small number of similar-sized garnet grains [7]. The latter approach was performed on granulitic garnet grains of high temperature of ~760 °C. At such high metamorphic temperatures, diffusional re-equilibration eliminates evidence of the early nuclei or growth.

Thus far, no study has revealed the correlation between garnet core Mn concentrations and Lu–Hf dates of individual garnet crystals in a metamorphic rock. Therefore, this study performs a systematic Lu–Hf radiometric study on single garnets of different sizes from a micaschist. The goal is to test the hypothesis that the Mn concentrations in the garnet core and the Lu–Hf dates of the garnet grains in low-temperature metamorphic rocks are correlated. Garnets extracted from a micaschist from the North Qilian orogenic belt at the northern edge of the Tibetan Plateau were selected due to the ease of extracting intact garnet crystals from the half-weathered hand specimen and the well-documented evolution history of the metamorphic rocks in the area, which appears to record a single metamorphic event.

2. Geological Background and Samples

The Qilian orogenic belt belongs to the Qilian–Qaidam orogeny in the northern Tibetan Plateau (Figure 1). Based on previous studies, the Qilian orogenic belt can be divided into five tectonic units from south to north: (a) the Qaidam block, (b) the North Qaidam UHP belt, (c) the Qilian block, (d) the North Qilian orogenic belt, and (e) the Alxa block [8]. The North Qilian orogenic belt represents an Early Paleozoic suture, separating the Qilian block in the south from the Alxa block in the north. The North Qilian orogenic belt, a typical oceanic-type suture zone, comprises ophiolitic mélanges, high-pressure and low-temperature meta-mafic rocks, island-arc volcanic rocks, granite plutons, and Silurian flysch formations. Previous studies on lawsonite-bearing eclogites and high-pressure blueschists of oceanic island basalt (OIB), mid-ocean ridge basalt (MORB), or island arc basalt origins suggest subduction of the "cold" oceanic lithosphere during the Paleozoic [5,8]. Zircon U–Pb ages for eclogites range from 463–479 Ma [5,8] and are interpreted to reflect eclogite-facies metamorphism. Recent garnet Sm–Nd and Lu–Hf ages for eclogites suggest that the initial subduction of the fossil Qilian oceanic basin may be traced back prior to *c.* 469 Ma, and its ultimate closure was earlier than *c.* 452 Ma [5].

These low-temperature and high-pressure metamorphic rocks are outcropped as blocks and pods (<~50 m in diameter) within metasediments in the North Qilian orogenic belt. The majority of the metasedimentary rocks are garnet-bearing micaschists. The micaschist sample studied in this contribution was collected at the Baishiyagou valley, approximately 30 km southeast of the Qilian Country (Figure 1). Several published contributions have presented detailed petrographic descriptions of these samples [9,10]. The present study focuses on the garnet-size effect on the Lu–Hf geochronology based on the highly weathered sample. Thus, we present less petrological descriptions below. We chose

the highly weathered rock chip to feasibly extract intact individual garnet crystals from the matrix. The mica schist sample shows a porphyroblastic texture and mainly contains garnet porphyroblast (10%), quartz (40%), muscovite (20%), biotite (10%), plagioclase (5%), and chlorite (3%) with minor rutile and monazite (Figure 1). Porphyroblastic garnets are 0.1–9.0 mm in diameter and are mostly half-imbedded (due to weathering) in a foliated matrix of muscovite–quartz–biotite plagioclase. Peak P – T metamorphic conditions were estimated from 430 to 560 °C and 9 to 14 kbar [9–11].

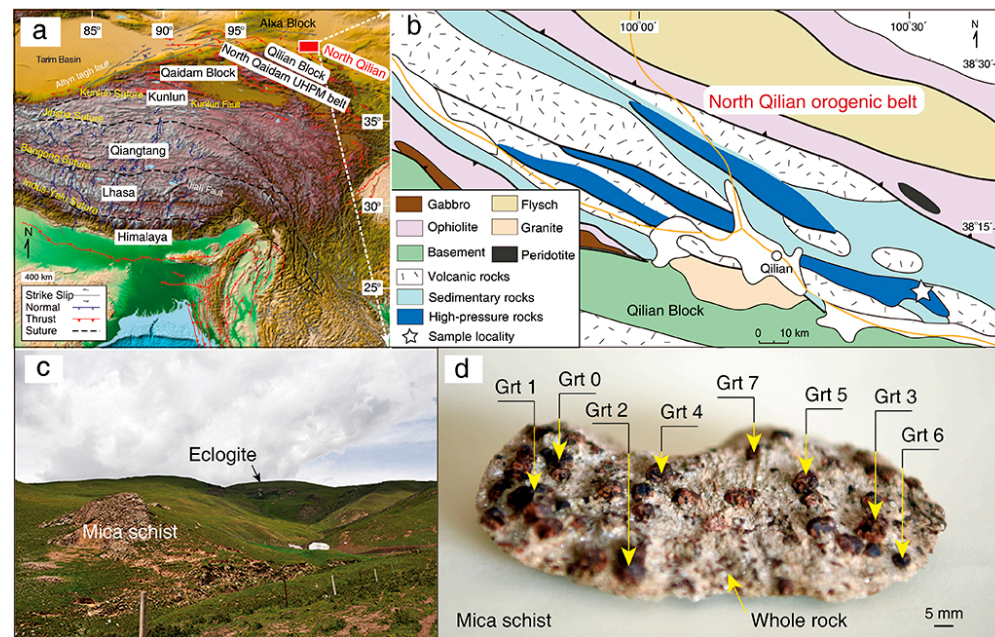


Figure 1. (a–c) Tectonic framework and geological map of the study area (after Cheng et al., 2018 [5]), showing the field occurrence of the sample in the North Qilian mica at the Baishiyazi valley. (d) A photograph of the highly weathered sample shows the extracted garnet grains for geochronology.

3. Methods

The sample was carefully crushed using a boron carbide mortar and pestle to liberate the individual garnet crystals from the mica-rich matrix in order to extract single garnet grains. Some grains, outcropped from the matrix rock chips, were extracted using long-nose pliers. Six intact garnet crystals of distinct sizes and several biotite grains were mounted in epoxy and polished down to expose the approximate geometric centers for electron probe analysis. The major element concentrations of the minerals were obtained using an electron microprobe (JEOL JXA-8230) at Tongji University equipped with five wavelength-dispersive (WDS) detectors. The beam conditions for the point analyses were 20 nA at 15 kV using a focused spot. The calibration was performed using natural and certified synthetic mineral standards, and a ZAF correction procedure was applied. The garnet rare earth element abundances were measured using an LA-ICP-MS at the State Key Laboratory of Marine Geology at Tongji University. The instrument is an Agilent 7500 quadrupole ICPMS equipped with an ArF Excimer laser (193 nm). A spot size of 32 μm was applied. The external calibration was performed relative to NIST610 and BHVO-2G standards together with internal standardization (Si). The details on the offline data correction and quantitative calibration can be found in Cheng et al. (2020) [3].

After extracting the garnets from the sample, the remaining matrix rock chips that were primarily free of garnets were collected to represent a garnet-free bulk rock. Another seven intact garnet crystals of distinct sizes were chosen for further isotope analyses. To reduce the sample loss during crushing and to remove surface contamination, individual garnet grains were washed in a warm 1.0 M HCl ultrasonic bath for 10 min and washed two times with deionized water before being crushed with a boron carbide mortar and

pestle. All the crushed fragments and powders were checked and hand-picked using a binocular microscope to remove other visible minerals. The remains were collected to represent a single “bulk” garnet aliquot. The Lu–Hf isotope data were analyzed using the Neptune™ MC–ICP–MS in the State Key Laboratory of Marine Geology at Tongji University. The digestion and chromatographic separation steps for Sm, Nd, Lu, and Hf followed the procedures presented in detail in Li et al. (2022) [12]. An exponential law using $^{179}\text{Hf}/^{177}\text{Hf} = 0.7325$ was applied for the mass fractionation corrections. The $^{176}\text{Hf}/^{177}\text{Hf}$ ratios were normalized against the reference standard JMC475 ($^{176}\text{Hf}/^{177}\text{Hf} = 0.282160$) and an in-house Hf isotope reference (TJU-475; $^{176}\text{Hf}/^{177}\text{Hf} = 0.282237$; an ultrapure metal chunk from the Ames Laboratory). A 0.5% external uncertainty for $^{176}\text{Lu}/^{177}\text{Hf}$ was applied to the measured data for isochron regressions and age calculations. To estimate a more realistic uncertainty for the data used to generate the Lu–Hf isochron ages, a blanket uncertainty of 0.005% was propagated with the in-run errors from the Hf isotope analyses. The IsoplotR software [13] was used to regress the isochrons and calculate the isochron ages, applying $1.867 \times 10^{-11} \text{ yr}^{-1}$ for $\lambda^{176}\text{Lu}$ [14]. All uncertainties are reported at the 95% confidence level.

4. Results

4.1. Mineral Chemistry

The representative garnet exhibits strong chemical zoning with decreasing spessartine (XSps 0.26–0.06), increasing almandine (XAlm 0.61–0.78) from the core to the rim, and slightly increasing pyrope (XPrp 0.05–0.19) rimward (Figure 2; Table 1), typical of growth during progressive prograde metamorphism. Six garnets of different sizes show Mn-enriched and Fe-depleted cores and Mn-depleted and Fe-enriched rims (Table 2). These garnets have distinct core compositions that vary with the garnet size but show similar rim compositions, whereas the core spessartine contents generally increase with the garnet diameter (Figure 2). Representative electron microprobe analyses for biotite are provided in Table 3. Lu in the garnet generally shows Rayleigh-style growth zoning, characterized by high Lu concentrations in the inner cores that rapidly decrease towards the rims. (Figure 2; Table 4).

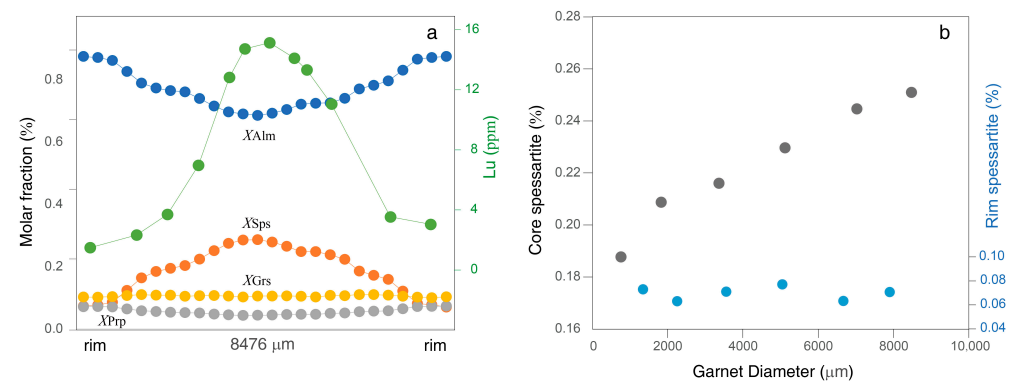


Figure 2. (a) Chemical zoning profiles of a representative garnet grain. (b) Garnet diameter plotted as a function of the core and rim Mn concentration, showing a correlation between the diameter and the core Mn compositions and similar rim Mn contents for different sized garnets.

Table 1. Rim-to-rim traverse electron analyses of a representative garnet ¹ (wt.%).

Posit. ²	317 ³	634	951	1267	1584	1901	2218	2535	2852	3168	3485	3802	4119
SiO ₂	36.88	36.79	36.84	36.63	36.67	36.43	36.99	36.63	37.09	36.45	36.82	36.85	36.32
TiO ₂	0.03	0.04	0.04	0.06	0.07	0.08	0.08	0.08	0.09	0.09	0.10	0.10	0.10
Al ₂ O ₃	21.10	21.09	20.85	20.94	20.98	21.07	21.15	20.80	21.23	21.23	20.86	20.66	20.80
FeO	33.84	33.57	33.35	31.95	30.27	29.60	29.58	29.71	28.47	27.43	26.67	26.51	26.14
MnO	2.77	2.89	3.25	4.71	6.17	6.95	7.41	7.83	8.49	9.49	10.37	10.79	10.77

Table 1. Cont.

Posit. ²	317 ³	634	951	1267	1584	1901	2218	2535	2852	3168	3485	3802	4119
MgO	1.54	1.54	1.51	1.37	1.24	1.19	1.15	1.13	1.08	1.02	0.96	0.92	0.92
CaO	3.07	3.05	3.11	3.22	3.28	3.21	3.26	3.17	3.19	3.19	3.13	3.06	3.12
Total	99.24	98.96	98.95	98.88	98.68	98.53	99.61	99.35	99.64	98.89	98.91	98.90	98.18
Oxygens	12	12	12	12	12	12	12	12	12	12	12	12	12
Si	3.00	3.00	3.01	3.00	3.00	2.99	3.00	3.00	3.01	2.99	3.02	3.02	3.00
Al	2.02	2.03	2.01	2.02	2.03	2.04	2.02	2.00	2.03	2.05	2.01	2.00	2.03
Ti	0.00	0.00	0.00	0.00	0.00	0.00	0.01	0.00	0.01	0.01	0.01	0.01	0.01
Fe ³⁺	0.00	0.00	0.00	0.00	0.00	0.00	0.00	0.00	0.00	0.00	0.00	0.00	0.00
Fe ²⁺	2.30	2.29	2.28	2.19	2.07	2.03	2.01	2.03	1.93	1.88	1.83	1.82	1.81
Mn	0.19	0.20	0.23	0.33	0.43	0.48	0.51	0.54	0.58	0.66	0.72	0.75	0.75
Mg	0.19	0.19	0.18	0.17	0.15	0.15	0.14	0.14	0.13	0.12	0.12	0.11	0.11
Ca	0.27	0.27	0.27	0.28	0.29	0.28	0.28	0.28	0.28	0.28	0.27	0.27	0.28
Sum	7.98	7.98	7.99	7.99	7.98	7.99	7.98	8.00	7.97	7.99	7.97	7.98	7.98
X _{Alm}	0.78	0.78	0.77	0.74	0.71	0.69	0.68	0.68	0.66	0.64	0.62	0.62	0.61
X _{Sps}	0.06	0.07	0.08	0.11	0.15	0.16	0.17	0.18	0.20	0.22	0.24	0.25	0.26
X _{Prp}	0.06	0.06	0.06	0.06	0.05	0.05	0.05	0.05	0.04	0.04	0.04	0.04	0.04
X _{Grs}	0.09	0.09	0.09	0.10	0.10	0.10	0.10	0.09	0.09	0.10	0.09	0.09	0.09
Posit. ²	4436	4753	5070	5386	5703	6020	6337	6654	6971	7287	7604	7921	8238
SiO ₂	36.15	36.28	36.93	36.43	36.70	36.60	37.03	36.97	36.33	36.33	36.87	36.60	37.27
TiO ₂	0.10	0.10	0.09	0.09	0.09	0.08	0.08	0.07	0.07	0.05	0.04	0.04	0.03
Al ₂ O ₃	20.84	20.99	21.31	20.88	21.09	20.53	21.05	20.87	20.91	21.06	20.94	20.71	21.17
FeO	26.35	26.79	27.81	28.12	27.61	28.36	29.48	29.86	30.69	32.27	33.36	33.66	33.63
MnO	10.47	9.94	9.42	9.48	8.94	8.43	6.99	6.47	6.03	4.61	3.08	2.94	2.64
MgO	0.94	0.98	1.01	1.00	1.05	1.09	1.17	1.21	1.24	1.40	1.53	1.55	1.57
CaO	3.12	3.12	3.14	3.08	3.18	3.17	3.27	3.26	3.24	3.16	3.05	3.01	3.07
Total	97.96	98.20	99.70	99.09	98.65	98.26	99.07	98.70	98.52	98.88	98.86	98.49	99.39
Oxygens	12	12	12	12	12	12	12	12	12	12	12	12	12
Si	2.99	2.99	3.00	2.99	3.01	3.02	3.02	3.02	2.99	2.98	3.01	3.01	3.02
Al	2.03	2.04	2.04	2.02	2.04	2.00	2.02	2.01	2.03	2.03	2.02	2.01	2.02
Ti	0.01	0.01	0.01	0.01	0.01	0.01	0.00	0.00	0.00	0.00	0.00	0.00	0.00
Fe ³⁺	0.00	0.00	0.00	0.00	0.00	0.00	0.00	0.00	0.00	0.01	0.00	0.00	0.00
Fe ²⁺	1.82	1.85	1.89	1.93	1.89	1.96	2.01	2.04	2.11	2.21	2.28	2.31	2.28
Mn	0.73	0.69	0.65	0.66	0.62	0.59	0.48	0.45	0.42	0.32	0.21	0.20	0.18
Mg	0.12	0.12	0.12	0.12	0.13	0.13	0.14	0.15	0.15	0.17	0.19	0.19	0.19
Ca	0.28	0.28	0.27	0.27	0.28	0.28	0.29	0.29	0.29	0.28	0.27	0.26	0.27
Sum	7.99	7.98	7.98	8.00	7.97	7.98	7.97	7.97	7.99	8.00	7.98	7.99	7.97
X _{Alm}	0.62	0.63	0.64	0.65	0.65	0.66	0.69	0.70	0.71	0.74	0.77	0.78	0.78
X _{Sps}	0.25	0.24	0.22	0.22	0.21	0.20	0.17	0.15	0.14	0.11	0.07	0.07	0.06
X _{Prp}	0.04	0.04	0.04	0.04	0.04	0.05	0.05	0.05	0.05	0.06	0.06	0.06	0.07
X _{Grs}	0.09	0.09	0.09	0.09	0.10	0.09	0.10	0.10	0.10	0.09	0.09	0.09	0.09

¹ $X_{Alm} = Fe^{2+} / (Fe^{2+} + Mn + Mg + Ca)$, $X_{Prp} = Mg / (Fe^{2+} + Mn + Mg + Ca)$, $X_{Sps} = Mn / (Fe^{2+} + Mn + Mg + Ca)$, $X_{Grs} = Ca / (Fe^{2+} + Mn + Mg + Ca)$. Recalculation of Fe³⁺ was based on stoichiometry and charge balance. ² Garnet in Figure 1d (Grt 0). Distance away from the rim (μm). ³ Used in the garnet–biotite thermometer calculation.

Table 2. Representative electron microprobe analyses for six garnet grains of the micaschist (wt.%).

No. ¹	Grt 1 (8476)		Grt 2 (7029)		Grt 3 (5121)		Grt 4 (3367)		Grt 5 (1831)		Grt 6 (765)	
	Core	Rim ²	Core	Rim ²								
SiO ₂	36.48	36.75	36.70	37.25	36.64	36.64	36.83	36.72	36.76	36.78	36.92	36.76
TiO ₂	0.10	0.04	0.10	0.03	0.09	0.04	0.09	0.04	0.09	0.03	0.08	0.04
Al ₂ O ₃	20.97	21.10	20.66	21.16	21.02	21.03	21.19	20.96	21.21	20.89	21.14	20.90
FeO	26.74	33.63	26.79	34.04	27.35	33.28	27.81	33.96	28.17	33.60	28.91	33.75
MnO	10.71	3.03	10.41	2.66	9.76	3.35	9.17	3.08	8.88	2.62	8.00	3.16
MgO	0.93	1.53	0.97	1.56	0.98	1.53	1.04	1.54	1.05	1.58	1.11	1.53
CaO	3.10	3.04	3.16	3.07	3.16	3.13	3.17	3.11	3.19	3.13	3.25	3.07
Total	99.02	99.11	98.78	99.79	99.01	98.99	99.30	99.40	99.35	98.63	99.41	99.21
Oxygens	12	12	12	12	12	12	12	12	12	12	12	12
Si	2.99	3.00	3.01	3.01	3.00	2.99	3.00	2.99	3.00	3.01	3.00	3.00
Al	2.03	2.03	2.00	2.02	2.03	2.03	2.03	2.01	2.04	2.02	2.03	2.01
Ti	0.01	0.00	0.01	0.00	0.01	0.00	0.01	0.00	0.01	0.00	0.01	0.00
Fe ³⁺	0.00	0.00	0.00	0.00	0.00	0.00	0.00	0.00	0.00	0.00	0.00	0.00
Fe ²⁺	1.83	2.29	1.84	2.30	1.87	2.27	1.90	2.32	1.92	2.30	1.97	2.30
Mn	0.74	0.21	0.72	0.18	0.68	0.23	0.63	0.21	0.61	0.18	0.55	0.22
Mg	0.11	0.19	0.12	0.19	0.12	0.19	0.13	0.19	0.13	0.19	0.14	0.19
Ca	0.27	0.27	0.28	0.27	0.28	0.27	0.28	0.27	0.28	0.27	0.28	0.27
Sum	7.99	7.99	7.98	7.98	7.98	7.99	7.98	8.00	7.98	7.98	7.98	7.99
X _{Alm}	0.62	0.78	0.62	0.78	0.64	0.77	0.65	0.78	0.65	0.78	0.67	0.77
X _{Sps}	0.25	0.07	0.24	0.06	0.23	0.08	0.22	0.07	0.21	0.06	0.19	0.07
X _{Prp}	0.04	0.06	0.04	0.06	0.04	0.06	0.04	0.06	0.04	0.07	0.05	0.06
X _{Grs}	0.09	0.09	0.09	0.09	0.09	0.09	0.09	0.09	0.09	0.09	0.10	0.09

¹ Garnets in Figure 1d (Grt 1–6). Numbers in brackets indicate diameters (μm). ² Used in the garnet–biotite thermometer calculation.

Table 3. Representative electron microprobe analyses for three biotite grains in contact with the garnet (wt.%).

No. ¹	Bt 1-Core	Bt 2-Core	Bt 3-Core
SiO ₂	35.12	34.81	35.26
TiO ₂	1.38	1.48	1.58
Al ₂ O ₃	19.76	19.77	20.10
FeO	13.58	13.21	13.38
MnO	0.04	0.02	0.04
MgO	17.34	17.12	17.24
CaO	0.02	0.01	0.01
Na ₂ O	0.32	0.36	0.32
K ₂ O	8.78	8.79	8.87
Total	96.38	95.63	96.89
Oxygens	11	11	11
Si	2.55	2.55	2.55
Al	0.08	0.08	0.09
Ti	1.69	1.71	1.71
Fe ³⁺	0.12	0.12	0.12
Fe ²⁺	0.70	0.69	0.69
Mn	0.00	0.00	0.00
Mg	1.88	1.87	1.86
Ca	0.00	0.00	0.00
Na	0.05	0.05	0.05
K	0.81	0.82	0.82
Sum	7.89	7.89	7.88

¹ Each analysis was paired with the garnet compositions in Tables 1 and 2 for the garnet–biotite thermometer calculation.

Table 4. Rim-to-rim rare earth elements data of a representative garnet (ppm).

Posit. ¹	387	1073	1760	2446	3133	3819	4506	5192	5879	6565	7252	7938
La	0.00	0.04	0.02	0.03	0.03	0.04	0.02	0.03	0.02	0.02	0.02	0.02
Ce	0.02	0.07	0.04	0.12	0.19	0.17	0.00	0.00	0.00	0.06	0.04	0.05
Pr	0.01	0.03	0.03	0.02	0.02	0.01	0.00	0.00	0.00	0.01	0.00	0.01
Nd	0.06	0.12	0.18	0.11	0.15	0.11	0.06	0.06	0.00	0.08	0.08	0.04
Sm	0.26	0.27	0.23	0.23	0.41	0.32	0.38	0.36	0.18	0.40	0.13	0.14
Eu	0.28	0.28	0.26	0.30	0.25	0.24	0.31	0.39	0.34	0.36	0.24	0.31
Gd	3.77	5.42	6.60	6.75	6.78	6.89	6.68	6.49	6.27	5.80	5.58	5.58
Tb	1.12	1.48	1.68	1.86	1.94	2.05	2.02	1.80	1.78	1.56	1.20	1.08
Dy	9.18	11.69	11.87	15.91	17.13	18.94	17.97	15.92	15.13	11.29	9.20	8.53
Ho	2.89	4.03	4.49	4.19	4.92	4.66	4.94	5.09	4.73	3.47	3.12	2.79
Er	11.1	11.5	15.2	19.3	21.6	21.5	22.5	22.4	21.8	19.6	15.3	11.4
Tm	2.29	2.91	3.81	4.34	5.15	5.35	5.69	5.82	5.76	5.10	3.77	3.34
Yb	13.5	21.7	31.0	47.5	64.9	66.9	70.6	73.9	72.1	55.7	33.9	27.5
Lu	1.49	2.33	3.70	6.97	12.83	14.72	15.13	14.11	13.32	11.05	3.54	3.04

¹ Garnet in Figure 1d (Grt 0). Distance away from the rim (μm).

4.2. Lu–Hf Isotopic Data

The Lu–Hf isotopic results are listed in Table 5. The Lu–Hf isochrons are shown in Figure 3. The parent/daughter ratios of Lu/Hf for the garnets are 8.2–9.9. These high parent-to-daughter (p/d) ratios suggest minor contamination of low p/d inclusions, for example, zircon (Hf), for these garnets. Seven garnet fractions combined with the whole-rock aliquot yield two-point isochron dates from 479 ± 3 Ma to 463 ± 3 Ma (Figure 3). A regression including only garnets produces a mixture line with an apparent date of 556 ± 18 Ma (MSWD = 0.32, $p(\chi^2) = 0.9$; Figure 4), which is statistically precise yet geologically meaningless. Great caution should be taken when interpreting mineral internal isochrons. The date obtained for each garnet grain decreases with grain size (Figure 5).

Table 5. Lu–Hf isotope data for the seven garnets and the whole rock.

Sample ^a	Dia ^b	Lu (ppm)	Hf (ppm)	¹⁷⁶ Lu/ ¹⁷⁷ Hf ^c	¹⁷⁶ Hf/ ¹⁷⁷ Hf	±2σ ^d	Age (Ma)
WR		0.356	1.059	0.0477	0.282561	15	
Grt 1	9143	5.033	0.506	1.413	0.294821	16	479 ± 3
Grt 2	8529	4.987	0.536	1.323	0.293938	16	476 ± 3
Grt 3	7023	4.187	0.461	1.292	0.293597	17	473 ± 3
Grt 4	6657	4.104	0.457	1.276	0.293406	17	471 ± 3
Grt 5	6521	3.979	0.448	1.264	0.293288	17	470 ± 3
Grt 6	5889	3.179	0.380	1.190	0.292507	17	464 ± 3
Grt 7	5764	3.077	0.375	1.165	0.292256	17	463 ± 3

^a Grt, garnet fraction; WR, whole rock without garnet. ^b Garnet diameter as in microns. ^c A 0.5% external uncertainty was applied to the measured data for regressions and age calculations. ^d Reported errors are based on the within-run errors and external reproducibility of the standards.

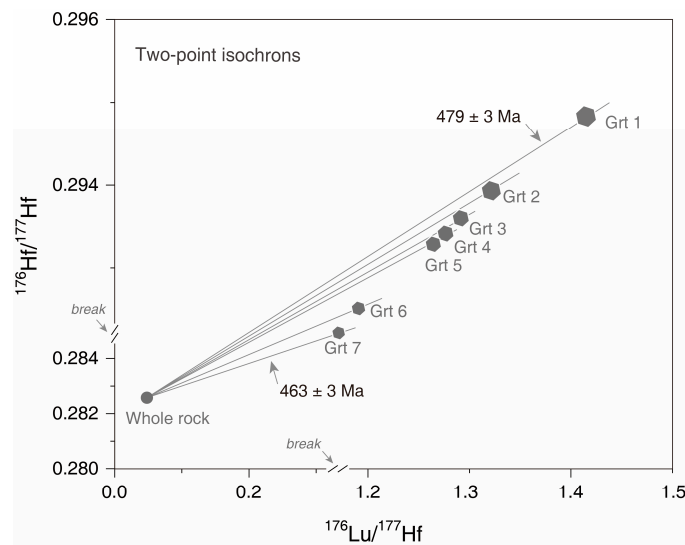


Figure 3. Lu–Hf isochron diagram for seven garnet and whole-rock aliquots. Two breaks are set in the X-axis and Y-axis to amplify the differences between the garnet fractions. The size of the symbols is significantly larger than the error bars.

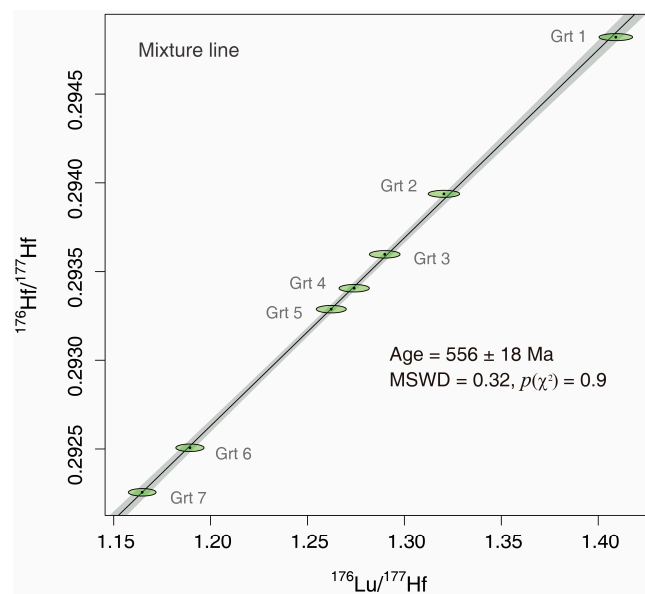


Figure 4. Mixture Lu–Hf errorchron diagram for the seven garnets.

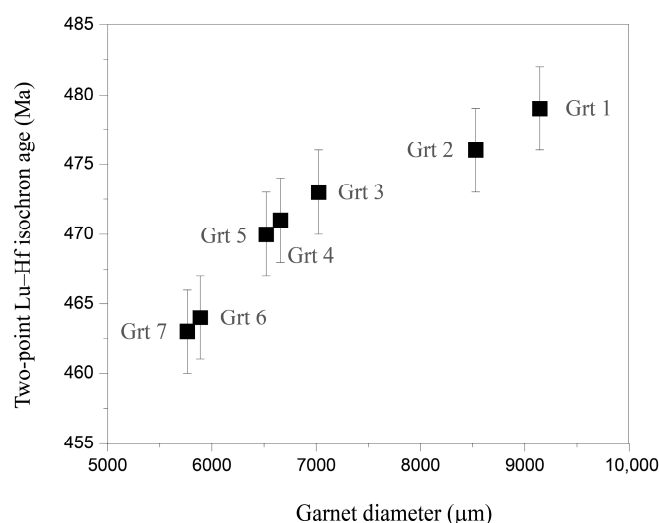


Figure 5. Correlation between the garnet diameters and the corresponding Lu–Hf date.

5. Discussion

5.1. Garnet Age Interpretations

During metamorphic garnet growth, certain elements, such as Mn and Lu, are preferentially incorporated into the growing crystal. As such, chemically zoned porphyroblast garnet is produced due to the progressively depleted garnet-preferred elements in the matrix as more minerals nucleate and grow. These chemical variations in metamorphic garnets are viewed as a proxy for the spatial and temporal scales of progressive metamorphism [15]. Given the well-observed correlations between garnet sizes and core Mn compositions, numerous studies suggest that it is reasonable to utilize Mn zoning as a proxy for garnet nucleation and growth during thermal evolution [15,16] as long as diffusive re-equilibration is insignificant. If the garnet growth spanned a long time interval, the core-versus-rim fractionation of Lu [17] would result in a correlation between the garnet sizes and single garnet Lu–Hf ages.

The positive correlation between the core Mn contents and garnet diameters (Figure 2) indicates that garnets with high-Mn cores nucleated first and preserved a longer record of the metamorphism as compared to garnets characterized by low-Mn core compositions that most likely crystallized later in the metamorphic history. The peak metamorphic temperature was calculated using the Ti-in-biotite [18] and the garnet–biotite thermometers [19]. The temperature was estimated using the compositions of the garnet rims in contact with biotite and high-Ti content biotite, yielding a range of 467–524 °C (Tables 2 and 3). This is in agreement with previous estimates [9,10]. Therefore, the diffusional re-equilibration at such metamorphic temperatures is negligible [15], and the chemical zoning in the garnet faithfully records the progressive metamorphic history.

The chemically zoned garnets in the matrix show evidence of non-equilibrium growth. However, it is believed that chemical equilibrium was maintained between the growing garnet rims and the matrix during changes in the metamorphic conditions [20]. This is supported by similar rim compositions for garnets of different sizes (Figure 2). Therefore, the nucleation and growth of the different-sized garnets in this sample were likely continuous. The two-point isochron, obtained from the bulk single garnet, reflects an average time interval of the overall garnet growth. The bell-shaped Lu zoning (Figure 2) indicates that the Lu–Hf date reflects garnet growth and skews to earlier growth stages. The correlation between garnet diameters, core Mn contents, and the age variation resulting from diachronous nucleation supports the conclusion that the observed age range represents the total garnet growth time span. Therefore, the larger the garnet crystal is, the earlier and over a longer time period it records. Garnets of different sizes provide snapshots of the overall garnet growth interval, as evidenced by the statistically robust mixture line defined by the seven individual garnet samples (Figure 4) with a low mean square of weighted

deviation (MSWD = 0.32) and high chi-squared value ($\chi^2 = 0.9$). Therefore, the oldest age of 479 ± 3 Ma obtained from the largest garnet should be considered a minimum estimate of the initial garnet growth during the prograde metamorphic process. The youngest age of 463 ± 3 Ma obtained from the smallest garnet implies that the garnet growth at peak metamorphism terminated no earlier than ca. 463. The 16 ± 4 Myr difference between the maximum and minimum ages determined by the largest and smallest garnet grains represents a minimum duration for the overall growth process.

5.2. Tectonic Implications

The low peak metamorphic temperatures of the mafic blueschists and eclogites in the North Qilian require oceanic subduction and exhumation along a low geothermal gradient path [8]. Numerous U–Pb analyses on the zircon igneous cores of eclogites show scarce Cambrian dates with a statistic peak value of ca. 494 Ma [5], reflecting protolith age. Previous geochronological data on high-grade rocks [5,8–11] indicate that the subduction of the oceanic basin initiated at ca. 469 Ma, and its ultimate closure was no earlier than ca. 452 Ma in the North Qilian orogenic belt [5–11]. The limited time span from ca. 469–452 Ma was obtained from various high-pressure/low-temperature rocks of a large span of peak metamorphic conditions (~ 420 – 580 °C and ~ 1.4 – 2.4 GPa) [7,9,10]. We consider two end-member alternatives to explain the observed ages and P – T relationships. In one scenario, these high-grade rocks are from a single subducted coherent slab that underwent different depths of subduction. In the other scenario, these high-grade rocks belonged to distinct slabs. They experienced synchronous yet different prograde metamorphic paths, i.e., distinct P – T conditions, and were later exhumed together concurrently.

However, the oldest Lu–Hf date obtained from the largest garnet in the pelitic schist suggests that garnet growth initiated before ca. 479 Ma (Figure 3). This is ~ 10 Myr older than the oldest Lu–Hf date (ca. 469 Ma) for the eclogitic garnet in the North Qilian orogenic belt [5,11] and ~ 15 Myr younger than the protolith age (ca. 494 Ma) of the eclogite [5]. The youngest Lu–Hf date obtained from the smallest garnet in the pelitic schist suggests garnet growth terminated at approximately 463 Ma (Figure 3). Thus, the pelitic schist pre-dates (ca. 479–463 Ma) adjoining eclogites and blueschists (ca. 469–452 Ma), indicating that the pelitic schist and its enclosing eclogites and blueschists did not undergo simultaneous metamorphic processes. The age discrepancy could not be explained by the above-mentioned scenarios based on previous studies. Instead, a scenario in which the pelitic schists and eclogites/blueschists belonged to distinct slabs, experienced different prograde-peak metamorphic processes asynchronously, and juxtaposed during exhumation is the likely explanation for the age discrepancy. To reconcile the conflicting scenarios, further investigation is needed through more comprehensive petrological analysis, incorporating geochemical data and accurate dating of metasediments and metabasic rocks from various tectonic subblocks in the North Qilian orogenic belt.

Author Contributions: Conceptualization, H.C.; Investigation, H.C. and C.C.; Writing—original draft, H.C.; Writing—review and editing, H.C. and C.C. All authors have read and agreed to the published version of the manuscript.

Funding: This research received no external funding.

Data Availability Statement: All data used during the study appear in the article.

Acknowledgments: The authors thank L.M. Zhang for her assistance with the electron probe and K.Y. Du for her assistance with isotope geochemistry and mass spectrometry. We thank three anonymous reviewers for their thorough reviews, which substantially improved this manuscript.

Conflicts of Interest: The authors declare no conflict of interest.

References

1. Baxter, E.F.; Scherer, E.E. Garnet geochronology: Timekeeper of tectonometamorphic processes. *Elements* **2013**, *9*, 433–438. [[CrossRef](#)]
2. Kelly, E.D.; Carlson, W.D.; Connelly, J.N. Implications of garnet resorption for the Lu–Hf garnet geochronometer: An example from the contact aureole of the Makhavinekh Lake Pluton, Labrador. *J. Metamorph. Geol.* **2011**, *29*, 901–916. [[CrossRef](#)]
3. Cheng, H.; Bloch, E.; Moulas, E.; Vervoort, J.D. Reconciliation of discrepant U–Pb, Lu–Hf, Sm–Nd, Ar–Ar and U–Th/He dates in an amphibolite from the Cathaysia Block in Southern China. *Contrib. Mineral. Petrol.* **2020**, *175*, 1–17. [[CrossRef](#)]
4. Simpson, A.; Gilbert, S.; Tamblyn, R.; Hand, M.; Spandler, C.; Gillespie, J.; Nixon, A.; Glorie, S. In-situ Lu–Hf geochronology of garnet, apatite and xenotime by LA ICP MS/MS. *Chem. Geol.* **2021**, *577*, 120299. [[CrossRef](#)]
5. Cheng, H.; Zhou, Y.; Du, K.Y.; Zhang, L.M.; Lu, T.Y. Microsampling Lu–Hf geochronology on mm-sized garnet in eclogites constrains early garnet growth and timing of tectonometamorphism in the North Qilian orogenic belt. *J. Metamorph. Geol.* **2018**, *36*, 987–1008.
6. Tual, L.; Smit, M.A.; Cutts, J.; Kooijman, E.; Kielman-Schmitt, M.; Majka, J.; Foulds, I. Rapid, paced metamorphism of blueschists (Syros, Greece) from laser-based zoned Lu–Hf garnet chronology and LA-ICPMS trace element mapping. *Chem. Geol.* **2022**, *607*, 121003. [[CrossRef](#)]
7. Smit, M.A.; Scherer, E.E.; Mezger, K. Lu–Hf and Sm–Nd garnet geochronology: Chronometric closure and implications for dating petrological processes. *Earth Planet. Sci. Lett.* **2013**, *381*, 222–233. [[CrossRef](#)]
8. Song, S.G.; Niu, Y.L.; Su, L.; Xia, X.H. Tectonics of the North Qilian orogen, NW China. *Gondwana Res.* **2013**, *23*, 1378–1401. [[CrossRef](#)]
9. Song, S.G.; Zhang, L.F.; Niu, Y.L.; Wei, C.J.; Liou, J.G.; Shu, G.M. Eclogite and carpholite-bearing meta-pelite in the North Qilian suture zone, NWChina: Implications for Paleozoic cold oceanic subduction and water transport into mantle. *J. Metamorph. Geol.* **2007**, *25*, 547–563. [[CrossRef](#)]
10. Wei, C.J.; Song, S.G. Chloritoid–glaucofane schist in the north Qilian orogen, NW China: Phase equilibria and P-T path from garnet zonation. *J. Metamorph. Geol.* **2008**, *26*, 301–316. [[CrossRef](#)]
11. Cheng, H.; Lu, T.Y.; Cao, D.D. Coupled Lu–Hf and Sm–Nd geochronology constrains blueschist-facies metamorphism and closure timing of the Qilian Ocean in the North Qilian orogen. *Gondwana Res.* **2016**, *34*, 99–108. [[CrossRef](#)]
12. Li, X.-M.; Cheng, H.; Dragovic, B.; Du, K.-Y.; Zhou, Y. Multi-mineral petrochronology on a high-pressure mafic granulite reveals short-lived high-temperature metamorphism in the North China Craton. *J. Metamorph. Geol.* **2022**, *40*, 1447–1466. [[CrossRef](#)]
13. Vermeesch, P. IsoplotR: A free and open toolbox for geochronology. *Geosci. Front.* **2018**, *9*, 1479–1493. [[CrossRef](#)]
14. Söderlund, U.; Patchett, P.J.; Vervoort, J.D.; Isachsen, C.E. The ¹⁷⁶Lu decay constant determined by Lu–Hf and U–Pb isotope systematics of Precambrian mafic intrusions. *Earth Planet. Sci. Lett.* **2004**, *219*, 311–324. [[CrossRef](#)]
15. Carlson, W.D. The significance of intergranular diffusion to the mechanisms and kinetics of porphyroblast crystallization. *Contrib. Mineral. Petrol.* **1989**, *103*, 1–24. [[CrossRef](#)]
16. Spear, F.S. *Metamorphic Phase Equilibria and Pressure-Temperature-Time Paths*; Monograph, Mineralogical Society of America: Chantilly, Virginia, 1993; 799p.
17. Lapen, T.J.; Johnson, C.M.; Baumgartner, L.P.; Mahlen, N.J.; Beard, B.L.; Amato, J.M. Burial rates during prograde metamorphism of an ultra-high-pressure terrane: An example from Lago di Cignana, western Alps, Italy. *Earth Planet. Sci. Lett.* **2003**, *215*, 57–72. [[CrossRef](#)]
18. Henry, D.J.; Guidotti, C.V.; Thomson, J.A. The Ti-saturation surface for low-to-medium pressure metapelitic biotites: Implications for geothermometry and Ti-substitution mechanisms. *Am. Mineral.* **1995**, *90*, 316–328. [[CrossRef](#)]
19. Bhattacharya, A.; Mohanty, L.; Maji, A.; Sen, S.K.; Raith, M. Nonideal mixing in the phlogopite–annite binary: Constraints from experimental data on Mg–Fe partitioning and a reformulation of the biotite–garnet geothermometer. *Contrib. Mineral. Petrol.* **1992**, *111*, 87–93. [[CrossRef](#)]
20. Gatewood, M.P.; Dragovic, B.; Stowell, H.H.; Baxter, E.F.; Hirsch, D.M.; Bloom, R. Evaluating chemical equilibrium in metamorphic rocks using major element and Sm–Nd isotopic age zoning in garnet, Townshend Dam, Vermont, USA. *Chem. Geol.* **2015**, *401*, 151–168. [[CrossRef](#)]

Disclaimer/Publisher’s Note: The statements, opinions and data contained in all publications are solely those of the individual author(s) and contributor(s) and not of MDPI and/or the editor(s). MDPI and/or the editor(s) disclaim responsibility for any injury to people or property resulting from any ideas, methods, instructions or products referred to in the content.